

Design of Polyhydroxyalkanoate (PHA) Microbeads with Tunable Functional Properties and High Biodegradability in Seawater

Chloé Volant

University of South Brittany: Universite de Bretagne-Sud

Eric Balnois

University of Western Brittany: Universite de Bretagne Occidentale

Guillaume Vignaud

University of South Brittany: Universite de Bretagne-Sud

Anthony Magueresse

University of South Brittany: Universite de Bretagne-Sud

Stephane Bruzaud (✉ stephane.bruzaud@univ-ubs.fr)

University of South Brittany: Universite de Bretagne-Sud <https://orcid.org/0000-0002-4576-7681>

Research Article

Keywords: Polyhydroxyalkanoates, microbeads, surface properties, biodegradability, seawater

Posted Date: July 1st, 2021

DOI: <https://doi.org/10.21203/rs.3.rs-627889/v1>

License: © ⓘ This work is licensed under a Creative Commons Attribution 4.0 International License.

[Read Full License](#)

Version of Record: A version of this preprint was published at Journal of Polymers and the Environment on November 25th, 2021. See the published version at <https://doi.org/10.1007/s10924-021-02345-6>.

Design of polyhydroxyalkanoate (PHA) microbeads with tunable functional properties and high biodegradability in seawater

Chloé Volant^a, Eric Balnois^b, Guillaume Vignaud^a, Anthony Magueresse^a, Stéphane Bruzaud^{a*}

^a Institut de Recherche Dupuy de Lôme (IRDL), UMR CNRS 6027, Université Bretagne Sud, Rue St Maudé, 56100 Lorient, France

^b Laboratoire de Biotechnologie et Chimie Marines (LBCM), EA 3884, Université de Brest, Université de Bretagne Sud, Quimper, France

* E-mail address: stephane.bruzaud@univ-ubs.fr

Abstract

Commercial poly(3-hydroxybutyrate-co-3-hydroxyvalerate) (PHBHV) and poly(3-hydroxybutyrate-co-3-hydroxyhexanoate) (PHBHHx) were used to prepare microbeads, with diameter ranging from 50 to 100 μm , by an emulsion-evaporation process. The properties of the beads reveal that the elaboration process enables the formation of spherical particles, that the crystallinity of the former polymer is not altered during the process and that the surface roughness of the particles can be tuned by changing the nature of the lateral chain in the PHA structure, in good correlation with its crystalline behavior. The mechanical properties of the different PHA beads are also found to be intimately linked with the crystalline content of the beads, with modulus varying between 1 to 7 GPa. All these properties are also governing the degradation behavior of these materials, as tested under marine environment. With a rapid degradation, similar to cellulose, and a degradation rate correlated with the crystalline content,

these results emphasize the interest in developing PHA materials with tunable functions and degradation properties.

Keywords: Polyhydroxyalkanoates, microbeads, surface properties, biodegradability, seawater

1. Introduction

Microplastics are defined as solid plastic objects smaller than 5 mm in size, insoluble in water and not biodegradable [1]. Personal care products (PCPs) have been identified as a potential source of environmental pollution due to their high content in primary microplastics, with typical number and mass content about 2162 particles/g or 0.04 g/g [2-4]. According to the PCPs' consumption, approximately 1500 ton/year of micro plastics leach into the global aquatic environments, which account for 0.1% to 0.8 % of the annual global release of primary microplastics in the world oceans [2]. Until recently, PCPs products are mainly formulated with conventional microplastics such as polyethylene, polypropylene, poly(ethylene terephthalate) or poly(methylmethacrylate) [5-9]. In order to limit their impact on the marine environment, many countries have attempt to ban the presence of these microplastics in rinse-off cosmetic products (United States in 2015, France and South Korea in 2016, Canada and New Zealand in 2017) [10-12]. These laws and decrees have led manufacturers to develop sustainable solutions with the use of particles or beads, for example in exfoliation products, such as natural organic ingredients including plant or fruits hulls, kernels seeds, microcrystalline cellulose or the use of mineral particles such as silica or pumice stone [13, 14]. If these additives have the benefit to being natural and biodegradable materials compared to conventional polymers [15, 16], they nonetheless also present drawbacks because of their irregular shapes and size; they are generally colored, not or poorly stable in aqueous medium, with an inadequate hardness and their commercial quantity and availability are rather limited [17]. The cosmetic industry is thus interested in developing biodegradable particles in the micrometer size range for applications such as facial cleaning or scrub [5-8, 13, 42, 43] having a smoother action than natural crushed ingredients [18, 19].

Polyhydroxyalkanoates (PHA) which are bacterial polyesters produced by bacterial fermentation in particular in marine environment [20] are natural candidates for applications in cosmetic meeting

environmental constraints. In addition depending on the bacteria, stress conditions and substrates, a broad variety of PHA can be produced with different monomer units and thus leading to a variety of chemical and physical properties [18]. These properties can be modulated as a function of the chemical composition or length of the lateral chain, of the proportion of the monomer units and their distribution all along the polymer chain [19]. For example, Lemechko *et al.* [20] obtained poly(3-hydroxybutyrate-co-3-hydroxyvalerate) (PHBHV) macromolecules by optimizing the choice of carbon source (agro-ressources effluents) and the amount of valeric acid to produce a range of polymers with a controlled proportion of each monomer. The thermal properties showed a decrease of enthalpy of fusion as the hydroxyvalerate unit (HV) content increases. By increasing the proportion of HV monomer (from 5% up to 20%), the PHBHV polymer becomes more ductile with a decreasing of the glass transition temperature (T_g) and crystalline rate [21]. Poly(3-hydroxybutyrate-co-3-hydroxyhexanoate) (PHBHHx) is another kind of commercially available PHA. The substitution of the hydroxyvalerate unit by an hexanoate unit (HHx) induces changes in the polymer properties, the polymeric material becomes more ductile and stiffer [22, 23]. The T_g parameter is also affected by varying the rate and chemical structure of the unit of the copolymer [23]. For example, increasing the proportion of HHx from 7 to 18% decreases the glass transition temperature [24-26]. As a consequence of both phenomena, it has been reported that the degree of crystallinity, in the presence of HHx unit, becomes lower due to a disruption in the PHB crystal arrangement. The HHx unit generates a greater steric hindrance than HV units, the degree of crystallinity varies from 54% (with 5% HV) to 27% (with 7% HHx) [27]. Furthermore the crystalline rate of PHBHHx also decreases as the percentage of HHx unit increases from 4 to 20%, some authors have noted a decrease of 41 to 25% [26], while others have measured a decrease of 64 to 3% [28].

Several methods have been described for the production of biopolymers microparticles [29, 30] such as emulsification, gelation, drying, coacervation or precipitation. The choice of the method and then of the proceeding and formulation parameters influence the physico-chemical characteristics of the particles such as the porosity, sphericity, size, dispersity, surface appearance or shape of the particles [31-36]. The type of polymer, in particular its botanical origin, affects the size of the so-formed microparticles.

This has been demonstrated for starch-based particles obtained by nanoprecipitation [31]. The process of elaboration of the micro and nanoparticle is also a fundamental parameter that govern the final properties of the beads. For example, it has been shown that ultrasound process allows to obtain small PHB microbeads in comparison with a stirring process, with diameter of 0.14 μm and 32 μm respectively [32]. The size and sphericity are also influenced by the choice of solvent. For example, dichloromethane allows to obtain more homogeneous PHBHV microbeads than chloroform (0.8-7 μm and 0.1-0.4 μm) [33]. Other authors have shown that the size of PHBHV microbeads can be tuned by adjusting the surfactant concentration, obtaining a range of microbeads from 389 μm to 39 μm for 0.5 to 4% PVA [35]. The porosity of PHB-based microbeads is also found to be dependent on the amount of aqueous phase, used in an emulsification process [32]. The final process of the bead fabrication, the solvent evaporation process including the time and temperature, is also an important step in determining the final properties of the particles [32]. The biomedical domain is certainly the one that has contributed to the most significant results in the elaboration of PHA microparticles [37]. In a majority of studies on PHA particles, the emulsification process was developed to elaborate micrometer size particles made from PHBHV or PHBHHx polymer. **Table 1** sums up some of the main parameters used in these processes.

Table 1: List of the different parameters used to elaborate PHBHV or PHBHHx microparticles using the emulsification process and their applications. NS means not specified.

Type of polymer	Polymer solution	Surfactant solution	Stirring	Evaporation of the organic solvent	Microbeads size distribution, μm	Applications	References
PHBHV	5% w/v in chloroform	2% w/v aqueous PVA	Mechanical stirring (3000 rpm)	Mechanical stirring (800 rpm) for 4 to 7 h	21 μm	Encapsulation of andiroba oil	[38]
PHBHV	1.0% w/v in chloroform solution	1.0-3.0% w/v aqueous PVA	Mechanical stirring	Mechanical stirring at 300 rpm or 900 rpm,	3-30 μm	Encapsulation of coumarin-6 (C6) or pyrene (Py)	[36]

				continuously, for 24 h			
PHBHV	0.88-5.12 g mL ⁻¹ in chloroform	0.38-4.60% g.mL ⁻¹ aqueous PVA	Mechanical stirring	Mechanical stirring at 1400 rpm and for 4 h	4-19 µm	Encapsulation of flurbiprofen	[39]
PHBHV	2,5% w/v in chloroform	1% aqueous PVA	Mechanical stirring (1000 rpm)	Rotary evaporator	9 µm	Encapsulation of annatto extract	[40]
PHBHV	1% w/v in chloroform	2% (w/v) aqueous PVA	Mechanical stirring (1000-4000 rpm)	Vacuum distillation unit, and heated to 45 °C	10-300 µm	Encapsulation of trypan blue dye	[41]
PHBHV	2% w/v in dichloromethane	1% aqueous PVA (w/v)	Dropwise fashion	900 rpm for 8 h at room temperature with a 3-bladed propeller in an off-centre position	20-40 µm	Encapsulation of diazepam	[42]
PHBHV	0.05-0.20 g in 5 mL chloroform	1.0-1.2% aqueous PVA	Mechanical stirring (1000 rpm)	12 h at 25 °C	20-60 µm	Encapsulation of rifampicin	[43]
PHBHV	0.5% in chloroform	0-4 % w/v aqueous PVA	NS	700 rpm and 50°C for 6 hours	31-390 µm	Process effects on degradation in vitro	[35]
PHBHV	100 mg/mL chloroform	1-4 % w/v aqueous PVA	Mechanical stirring (500 rpm)	Nitrogen atmosphere was created in the flask and the solution was stirred until all the chloroform was evaporated.	322-538 µm	Encapsulation of tetracycline	[44]
PHBHHx	Dichloromethane	Aqueous SDS	NS	Magnetic stirring at room temperature	5-20 µm	Encapsulation of 5-fluorouracil or cyclosporin A	[45]

PHBHHx	0.1% w/v in acetone	ND	Vigorous stirring	Under vacuum at 35 °C overnight	75 μm	Effect of PHA particles on cell growth	[46]
--------	---------------------	----	-------------------	---------------------------------	-------	--	------

The objective of this work is to synthesize PHA microparticles for cosmetic applications with the following goals: size of approximately 100 μm, spherical shape particle with tunable surface aspect and mechanical properties and presenting good biodegradation properties in the marine environment. Surprisingly, to the best of our knowledge, the development of PHA microparticles for such application is poorly described. Three commercial PHA, of different chemical structures, were used to prepare microbeads by emulsion-evaporation process. The physico-chemical properties of the different beads were then studied, in terms of shape, crystallinity, surface and mechanical properties as well as biodegradability and compared with PLA microparticles used as control.

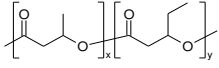
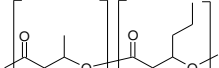
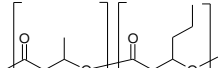
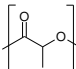
Among these 3 selected PHA, one (PHBHV) is readily available commercially while the other 2 (the both PHBHHx) are not. In these conditions, this prospective study will make it possible to consider expanding the range of applications of these PHA, especially for the both PHBHHx which are a new PHA kind, and find new potential uses for these PHA.

2. Materials and methods

2.1. Materials

Poly(3-hydroxybutyrate-co-hydroxyvalerate) (PHBHV) with 3 mol% in HV was supplied by Tianan Biological Materials Co. Ltd. (China), under the trade name ENMAT Y1000P. Poly(3-hydroxybutyrate-co-hydroxyhexanoate) (PHBHHx) with 6 mol% in HHx and PHBHHx with 11 mol % in HHx were supplied by Kaneka Corporation (Japan), under the trade name Aonilex X131A and Aonilex X151A, respectively. Polylactic acid (PLA) was purchased from NatureWorks under the trade name Ingeo 7001D. The physico-chemical properties of the investigated commercial polymers are given in **Table 2**. For clarification in the following text, the notation PHBHV, PHBHHx (6%) and PHBHHx (11%) and PLA will be used. All chemicals products and reagents used in these experiments were analytical grade and were purchased from Sigma-Aldrich.

117 **Table 2: Physico-chemical characteristics of PHBHV, PHBHHx (6% and 11% HHx) and PLA pellets**

Polymer	Chemical structure	Average molecular mass ($\times 10^3$ g mol ⁻¹)	PDI	X _c (%)	T _m (°C)	T _g (°C)	References
PHBHV (3% HV)		340-400	2.5-2.7	54-65	165-175	4-8	[27, 47]
PHBHHx (6% HHx)		345-452	1.9-2.6	27	142-145	2	[27] Technical sheet from Kaneka
PHBHHx (11% HHx)		550-614	2.0-2.4	34	126-136	0-2	[48-50] Technical sheet from Kaneka
PLA (4% D-lactide)		174-220	1.6-1.8	5	150-160	55-60	[51-54] Technical sheet from NatureWorks

119 2.2. Synthesis of biopolymers microparticles

120 Microparticules of PHBHV, PHBHHx (6% and 11%) and PLA were elaborated by emulsification
 121 process. PHBHV was dissolved at 50 g L⁻¹ in chloroform under reflux conditions (50 °C), PHBHHx and
 122 PLA were dissolved at the same concentration but in dichloromethane under reflux conditions (40 °C)
 123 during 24 hours. These polymer solutions were then slowly added in an aqueous solution of polyvinyl
 124 alcohol (2%) under mechanical stirring (4000 rpm). The emulsion time was fixed at 15 min. The
 125 particles were then dried by gently evaporating the solvent under continuous magnetic stirring during
 126 24 hours. The dried particles were collected by sequential sieving (Inox sieve with 250 µm and 50 µm
 127 mesh, Granuloshop, Chatou, France), washed several times with deionized water and lyophilized.

128 2.3. Characterization of the microparticles

129 2.3.1. Morphological analysis

130 The morphology of the microbeads was analyzed by a scanning electron microscope (JSM-IT500HR
 131 from JEOL). SEM observations were carried out with secondary electron detector at an acceleration
 132 voltage of 3 kV. The particles were stuck on adhesive carbon tape, then gold-coated using a sputter
 133 coater (Scancoat6 from Edwards). The quantitative determination of the microbeads diameter and their

shape was performed form image analysis following SEM observation. For each sample, a minimum of 500 microparticles were analyzed using ImageJ software (version 1.52, NIH) The circularity factor (CF) was determined using Equation (1):

$$CF = \frac{4\pi \times area}{(perimeter)^2} \quad (1)$$

The surface topographies of the microbeads were also evaluated by Atomic Force Microscopy (AFM). AFM measurements were obtained with a multimode 8 atomic force microscope (Bruker, Santa Barbara, CA) operated on the scanasyst@ mode (Bruker) under ambient conditions (23 °C, RH=50%). Standard scanasyst tips (Bruker), with a resonance frequency of 70 KHz and a spring constant of 0.4 N/m were used. Images were analyzed using the Nanoscope analysis software (V1.80). To ensure a good reproducibility in the measurements, for each sample, a minimum of three areas were investigated for each microbead, and for each sample a minimum of five different microbeads were observed.

2.3.2. Thermal properties

Thermal properties were analyzed by Differential Scanning Calorimetry (DSC). About 5-8 mg were introduced in standard aluminium pans, using Mettler-Toledo DSC882 equipment. Samples were heated from 25°C to 180°C at a scanning rate of 10°C min⁻¹ under nitrogen flow. Thermal characteristics were recorded such as transition temperatures (melting, crystallization and glass temperatures) and melting enthalpy (ΔH_m). Each sample was analyzed in triplicate.

2.3.3. Infra-red spectroscopy

Attenuated Total Reflection Fourier Transform Infrared (spectrophotometer ????) (ATR-FTIR Vertex70v, Bruker) was operated in the range from 4000 to 600 cm⁻¹ with 4 cm⁻¹ resolution. Dried microbeads were deposited directly on to the diamond crystal. For each sample, a minimum of 16 scans were performed to ensure a good reproducibility in the signals.

2.3.4. Nanomechanical properties

Nanoindentation experiments were obtained with a Nanoindenter XP from MTS Nano Instruments equipped with a three-side pyramid (Berkovich) indenter, as previously described [55]. All Experiments

were conducted under ambient conditions (23°C, RH 50%) and using the continuous stiffness measurement (CSM) method with the following parameters: 3 nm amplitude and 45 Hz oscillations using a 0.05 s^{-1} loading rate. Measurements were taken at depths to 1500 nm. A Poisson's ratio of 0 was used in all modulus calculations. For each sample, around 75 indents were performed with 5×5 matrix on different locations; average values of both elastic modulus and hardness were then calculated from curves according to the method of Oliver and Pharr [56]. Experiments were performed on polymer pellets included in an epoxy resin, polished prior experiments.

The AFM technique was also used to probe the nanomechanical properties of the polymer microbeads using the PeakForce Quantitative Nanomechanical Measurements (PFQNM). In PFQNM, the piezo of the AFM is vertically oscillating at a frequency of 2 kHz, with an amplitude of 150 nm. While the piezo move the sample beneath the tip in the X and Y direction, a force curve is recorded in every coordinate, allowing to extract mechanical properties from the materials. The spring constant of RTESP-525 commercial tips were evaluated using the Sader method (<https://sadermethod.org>) and the tip radius was determined using the relative calibration method. A polystyrene film of 2.7 GPa was used as a standard of calibration (PFQNM SPM kit-12M, Bruker). The peak force setpoint was typically set at 200 nN.

The indentation modulus was calculated using the Dejarguin-Muller-Toporov (DMT) model and extracted using the nanoscope image analysis software (V1.80). For each sample, a minimum of three areas were recorded and for each polymer, a minimum of three different bead were analyzed.

2.3.5. Biodegradability

Biodegradability of microbeads was determined with the NF EN ISO 19679 test that measures aerobic biodegradation of non-floating plastics at the seawater / sediment interface. The amount of total organic carbon contained in each sample ($m_{CO_2, theoretical}$) was determined by elemental analysis. The mass percentage is 44.44 ± 0.02 for micronized cellulose, 55.18 ± 0.02 for PHBHV, 56.52 ± 0.25 for PHBHHx (6%), 57.08 ± 0.18 for PHBHHx (11%) and 49.59 ± 0.17 for the PLA.

Sample preparation was previously described for solid/liquid state, as an adaptation of the Strum test [57]. Under continuous oxygenation in a sealed closed system, a first compartment contains the

microbeads in a mixture of seawater (100 mL) and sediment (30 g), and the second an absorbing solution with a NaOH solution (20 mL, 0.2 mol L⁻¹) and distilled water (20 mL). A blank flask with no sample is included in each test set up to determine the blank respiration of the seawater, as well as a standard composed of micronized cellulose to validate the results of the test. The test was carried out for 250 days in a water bath at 25 °C.

Since the produced carbon only comes from the biodegraded sample, the trapped CO₂ by the absorbing solution is proportional to the amount of carbon consumed. The product sodium carbonate by the reaction of CO₂ and NaOH is precipitated by a BaCl₂ solution. The remaining NaOH is titrating with hydrochloric acid (0.1 mol L⁻¹) to determine the CO₂ trapped by the absorbing solution. Rate of biodegradation (%CO₂) was determined from the Equation (2):

$$\%CO_2 = \frac{(m_{CO_2, sample} - m_{CO_2, control}) \times 100}{m_{CO_2, theoretical}} \quad (2)$$

Where $m_{CO_2, sample}$ is the amount of CO₂ produced in the sample test, $m_{CO_2, control}$ is the amount of CO₂ produced in blank test.

3. Results and discussion

3.1. Morphology of microbeads

SEM images of the different microbeads are presented in **Figure 1**. All the beads are spherical, as revealed by a circularity factor close to 1 (**Table 3**). The diameter of the beads (**Table 3**) is found to be dependent on the polymer nature, thus indicating that, for a similar elaboration process, using identical parameters, the chemical nature of the polymer controls the final size of the bead. PHBHV and PLA microbeads are the largest particles, with diameter around 100 µm, whereas PHBHHx particles have smaller diameters, that also decrease with a lower content in HHx. The large standard deviation measured on our samples may be associated with the elaboration process but also to the limited the number of particles measured by image analysis. These diameters are nonetheless consistent with other types of microparticles obtained using a similar process and determined by SEM or optical microscopy [16].

208 *Table 3: Mean diameter and circularity factor of the microparticles as determined from SEM image analysis. The average*
 209 *diameter and standard deviation were estimated on more than 500 particles.*

Microbeads	Microbeads size distribution (μm) (mean diameter \pm SD)	Circularity factor
PHBHV	94 ± 25	0.91
PHBHHx (6%)	48 ± 20	0.93
PHBHHx (11%)	75 ± 25	0.92
PLA	111 ± 42	0.93

210

211 From the SEM images, the surface roughness can be qualitatively observed. The SEM images at
 212 different resolution (**Figure 1**) reveals that the PLA bead is rather smooth in comparison with the rough
 213 surfaces of PHBHHx or PHBHV. The roughness was quantitatively estimated by means of the AFM,
 214 on area of approximately $25 \mu\text{m}^2$. It should be noted here that stable AFM images were difficult to
 215 obtained on larger scale ($> 25 \mu\text{m}^2$) due to instabilities generated by the topography on top of each bead
 216 and the variation in height imposed by the radius of curvature of the beads. **Figure 2** presents AFM
 217 images obtained of the top of the different beads and their corresponding surface analysis, confirming
 218 the smooth topography of the PLA beads and the important roughness of the PHA beads. At such scan
 219 size, the roughness between ~ 130 - 210 nm is obtained for the three PHA particles whereas a roughness
 220 of only 25 nm is obtained for the PLA. This observation is well correlated with the maximum height,
 221 R_{max} , measured on these images, showing the large distribution in height for the PHA particles (up to
 222 $1 \mu\text{m}$) and the relatively small height distribution for the PLA particle (200 nm). The roughness of the
 223 PHA particles can be associated with the semi-crystalline character of the polymer and fast precipitation
 224 induced by the rapid evaporation of the solvent. This trend was also reported in other studies but not
 225 quantified [58, 59]. Finally, it should also be mentioned, that considering scan area of $25 \mu\text{m}^2$, no
 226 differences in RMS can be attributed to the different PHA beads indicating that the crystallites of
 227 PHBHV and PHBHHx are forming similar surface structures on the periphery of the bead, considering
 228 the RMS and topographic point of view.

229 3.2. Thermal properties

The thermal properties of the four microbeads are reported in **Table 4**. Characteristic values are determined from the first heating to observe the effect of the elaboration process on the final properties of the beads. No difference can be observed between the thermal properties of the beads and of the original polymer pellets. PHA microbeads have a glass transition temperature around 0 °C. PHBHV exhibits one melting temperature at about 173 °C. Two melting peaks were detected for the PHBHHx sample, at 125 and 144 °C for PHBHHx (6%) and 109 and 137 °C for the PHBHHx (11%), attributed to the PHB segment melting temperature and to the PHHx segment melting temperature, respectively. These values are similar to the literature data [23, 24, 27, 39]. In contrast, PLA microbeads exhibits glass transition temperature around 60-63 °C, and a melting temperature of 147 °C. These results are also in good agreement with those described for amorphous PLA microbeads obtained by emulsion-evaporation in the presence of dichloromethane [33].

Table 4: Thermal characteristics of the different microbeads determined by DSC

Microbeads	T _g (°C)	T _m (°C)	ΔH _m (J/g) ^a
PHBHV	2.0 - 3.7	173	97
PHBHHx (6%)	1.9 - 2.3	125 and 144 ^b	56
PHBHHx (11%)	-1.1 - -0.5	109 and 137 ^b	40
PLA	60 - 63	147	22

^a Values of melting enthalpy, ΔH_m, are given as raw data and not converted into crystalline content because of the absence of reference for a PHA with 100 % crystallinity.

^b Two melting peaks were detected, one corresponding to PHB and the second one to HHx unit.

Thus, it can be concluded from these DSC analyses, that the elaboration process has no impact on the crystallization process of the PHA bead, as revealed by the SEM and AFM images. From these data, it appears that the most crystalline bead is the PHBHV sample. A difference in crystalline content can also be observed between the two PHBHHx samples, with the most crystalline bead being the 6% in HHx content. This data emphasizes the role of the chemical nature of lateral chain (HV vs HHx) in the PHA structure and in the final properties of the polymer material. The lateral chain may play the role of a plasticizer. For example, it has been demonstrated that increasing the fraction of HV monomers in PHBHV samples render the materials more ductile and less brittle, associated with a decrease in the melting and glass temperature proportionally [60]. Similarly, it has been shown that, increasing the

percentage of HHx from 7 to 18% results in a decrease in the crystallization rate and suppression of the spherulitic growth rate [24].

FTIR spectroscopy was performed in order to evaluate the surface crystallinity of the different beads. This technique is complementary with the DSC technique that give an overall estimation of the crystallinity, independently of the structural organization of the polymer within the bead and from the center of mass. FTIR, owing to the penetration depth of the IR beam of a about one micron [61], can be directly applied on the beads in contact with the ATR crystal and thus may give access to the polymer organization on its periphery, or close to it.

FTIR spectroscopy analysis were performed in order to get access to the surface crystallinity of the different beads. This technique is highly complementary with the DSC technique that give an overall estimation of the crystallinity, independently of the structural organization of the polymer within the bead and from the center of mass. FTIR is sensitive to the polymer organization on its periphery and within a thickness of a one micron approximatively. FTIR spectra of PHA microbeads are presented on **Figure 4**.

Figure 4 represents an IR spectrum of the PHA microbeads and reveals the different bands of interest for this polymer. The bands at 1230, 1380 and 1724 cm^{-1} are assigned to the crystalline part of the PHA sample whereas those at 1186 and 1741 cm^{-1} are representative of the amorphous part (see **Table 5A**). By comparing the intensities ratio of some of the characteristic bands of PHA, some authors were able to evaluate a crystallinity index and established a correlation between FTIR and DSC measurements [62, 63]. In the work of Xu *et al.* [62], the crystallinity index was calculated as the ratio of the crystalline band at 1380 cm^{-1} , assigned as the conformational band of helical chains in the crystalline phase, over the amorphous reference peak at 1453 cm^{-1} , assigned as methyl (CH_3) or methylene (CH_2) deformations [63]. In other studies, the crystallinity index of PHA samples was also evaluated by calculating the ratio of the absorbance peak at 1227 cm^{-1} over the absorbance peak at 1184 cm^{-1} [61], between the absorbance peak at 1724 cm^{-1} over the absorbance peak 1453 cm^{-1} [63], or between the absorbance peaks at 1380 cm^{-1} over the amorphous band at 1186 cm^{-1} [64].

Intensities of these ratio are reported in the **Table 5B**. The ratios of the crystalline peaks on to the amorphous peaks gives the highest ratio for the PHBHV bead, followed by the PHBHHx at 6% and 11% respectively. These results are in good agreements with the previous DSC results and confirms that the crystallinity on the surface of the particles is well correlated with the crystallinity content of the particles. The roughness parameter is also in good correlation with this finding.

Table 5A: identification of the representative FTIR peak for the different PHA samples

Frequency (cm ⁻¹)	Description	References
1741	stretching vibration of the amorphous carbonyl group	[61-63, 65, 66]
1724	stretching vibration of the crystalline carbonyl group	[61-63, 65, 66]
1453	methyl (CH ₃) or methylene (CH ₂) deformations in the amorphous phase	[63]
1380	symmetric wagging of CH ₃ in the crystalline phase	[61-63]
1227-1230	absorption of helical (α -type) crystals (C-O-C stretching modes of the crystalline components)	[61, 62, 67]
1184-1186	asymmetric C-O-C stretches (amorphous phase)	[61-63]

Table 5B: Comparison of the representative FTIR peak intensities ratios for the different PHA samples.

Microbeads	$\frac{I_{1380}}{I_{1186}}$	$\frac{I_{1230}}{I_{1453}}$	$\frac{I_{1227}}{I_{1184}}$
PHBHV	0.52	2.6	0.53
PHBHHx (6%)	0.27	1.21	0.28
PHBHHx (11%)	0.21	0.87	0.15

3.3. Mechanical properties

Nanoindentation measurements on the microbeads, with the MTS equipment, required their immobilization by an inclusion in an epoxy resin. However, due to their size and color, they were not clearly distinguishable on the surface of the resin. Furthermore, with an epoxy resin with a similar Young's modulus as the polymer beads (between 3-5 GPa), the experiment was not successful in

identifying correctly the polymer beads among the resin. Thus, nanoindentation test have been performed here directly on the pellets, even if a direct comparison with the bead materials should be cautious. In parallel to this nanoindentation experiments, PFQNM were realized directly on the top of the microbeads. With the AFM, it is easier to place the AFM tip on a top a bead to measure its mechanical properties locally.

Table 6 reports the values of the modulus for the different polymers pellets, as measured by nanoindentation. At first, the Young's modulus for PLA is found to be around 5.5 GPa, in good agreement with the literature value [68]. For the PHA samples, the two PHBHHx samples give the lowest Young's modulus as compared to the PHBHV. For the PHBHV polymer, a Young's modulus of 7.5 GPa has been found, similar to the measurements of Chick et al on injected PHBHV polymer [47]. The highest modulus found for the PHBHV sample can be related with its high crystalline content. In contrast, the PHBHHX samples shows the lowest Young's modulus, the 11% content in HHX monomer having the lowest modulus. These results are in good agreement with the recent work of Voyiadjis *et al.* [69], who studied the mechanical properties of PEEK semi-crystalline polymers. By varying the cooling rate of their sample, they vary the degree of crystallinity of their samples and observed a softer response of the amorphous polymer part as compared to the crystalline regions.

Table 6: Modulus and hardness of the different polymer materials (pellets) as measured by nanoindentation

Microbeads	Modulus (GPa)	Hardness (GPa)
PHBHV	6.9 ± 0.8	0.26 ± 0.06
PHBHHx 6%	2.8 ± 0.5	0.10 ± 0.02
PHBHHx 11%	1.7 ± 0.2	0.07 ± 0.01
PLA	5.6 ± 0.2	0.31 ± 0.02

Figure 5 represents the distribution in the indentation modulus for the different beads as measured by PFQNM. Results obtained are consistent with the moduli obtained by nanoindentation. One should observe nonetheless a slight increase in the modulus of the PHBHHx beads, measured by PFQNM as compared to the modulus of the pellets, obtained by nanoindentation. However, precautions should be

taken for an accurate determination of the modulus by PFQNM. At first, the calibration of the tip radius was performed on fairly flat Polystyrene film with a low roughness in comparison with the rough surface topographies of the different beads. Tip convolution effect is likely to occur, especially on rough surfaces as it is the case here and may result in different contact area which can affect the indentation modulus calculated from the force curve analysis. It has also been recently postulated that PFQNM experiments may provide slightly larger modulus as compared to other mechanical techniques, since the force curve may be partially impacted by the presence of adsorbed water that may increase the adhesion force between the tip and sample [70]. Nonetheless, the variation in the mechanical properties, as observed by the two techniques confirms that the bead present different mechanical properties, in correlation with their crystalline content and their chemical structure. Furthermore, it was found that the mechanical properties of the so-formed microparticles, following the described fabrication process, are comparable with the initial properties of the polymer pellets.

Finally, the hardness of the different samples was extracted from the nanoindentation measurements, as described by Oliver and Pharr [56]. The results, presented in **Table 6**, reveal that both PHBHHx samples have the lowest hardness in contrast with the PHBHV and PLA samples with a hardness around 0.3 GPa. Despite the PLA sample, the trend for PHA samples is also following the crystalline state of the different samples, the more crystalline being the more tough. For the PLA sample, which is less crystalline than the PHA sample, the mechanical properties can be correlated to its high glass transition in comparison with the PHA samples. It has been reported that the intrinsic stiffness of glassy polymers below the T_g may leads to microhardness values larger than those obtained for semi-crystalline polymers [71].

3.4. Stability in aqueous medium and biodegradability in marine environment

The stability of these particles in aqueous medium, with various conditions to mimic ageing conditions for cosmetic products (room temperature, room temperature in the presence of light and accelerated ageing at 45 °C) was verified by measuring the pH of the solution during a period of 3-months storage. The comparison between the PHA and PLA microbeads allows to observe different trends. On the one

hand, the pH variation for the solution containing the PHA microbeads was only slightly decreasing, with a pH variation inferior to 1 pH unit. For example, after 3 months at room temperature, pH of 3.9 for PHBHV, 3.7 for PHBHHx (6%) and 3.8 for PHBHHx (11%) were measured respectively in contrast with a starting pH of 4.2. Similar results were obtained when the PHA microbeads suspension was exposed to the 45°C thermostated aqueous solution (pH of 3.8, 3.6 and 3.7 for PHBHV, PHBHHx (6%) and PHBHHx (11%) respectively) and a more pronounced decreased of the pH, but still less than 1 pH unit, was recorded for the suspension in the solution at room temperature and exposed to light (pH of 3.5, 3.6 and 3.6 for PHBHV, PHBHHx (6%) and PHBHHx (11%) respectively).

On the other hand, the pH of the PLA suspension is decreasing of 1 pH unit for the normal aqueous solution conditions and aqueous solution plus light exposure conditions (from a pH = 4.4 down to a pH = 3.4) and by 2 pH unit for the 45°C aqueous solution conditions (from pH = 4.4 to pH = 2.4). The acidification of the PLA suspension can be correlated with a degradation of the polymer particles, showing that the PHA microparticles are less degradable and more stable under these conditions than PLA in aqueous medium.

The **Figure 6** shows the biodegradability of the different microbeads in seawater. The biodegradation has been performed on marine environment (seawater + sediments) at 25 °C, according to the NF EN ISO 19679 standard.

As expected, PLA microbeads are poorly biodegradable in these conditions since their biodegradation degree is only about 20% after 250 incubation days. It has been previously demonstrated that PLA is relatively stable, due to its glassy state at 25 °C, as long as the medium temperature does not exceed the PLA glass transition temperature, i.e. about 55 °C [72].

Concerning the PHA series, significant differences on the biodegradability can be noted depending on the chemical PHA structure. The PHBHV turns out to be the most biodegradable as its biodegradability percentage reaches to 90% after 250 days of immersion. For the PHBHHx, the composition of monomer units also influences the biodegradability since the PHBHHx with 11% in HHx biodegrades faster than the PHBHHx with 6% in HHx. The biodegradation rate is 80% for the first one and 62% for the second

one. It is very interesting to note in the **Figure 6** that all these PHA present a biodegradability greater than or close to that of the cellulose which is considered as a reference in terms of biodegradability. The beginning of the biodegradation is even faster for the 3 PHA compared to the cellulose.

This spectacular PHA biodegradability is explained the action of some marine microorganisms such as bacteria which excrete extracellular PHA degrading enzymes, i.e. PHA depolymerases, that hydrolyze water-insoluble PHA chains into water-soluble forms [73]. The resulting products are finally metabolized into the cells and utilized as nutriments [57]. At this temperature, the microbead degradation is therefore managed by an enzymatic degradation which is a heterogeneous surface reaction. Previous studies have revealed the presence of two PHA degradation mechanisms occurring in parallel (enzymatic degradation and chain scission by hydrolysis) but the enzymatic degradation is largely predominant at 25 °C in marine ageing conditions [72]. This process, whatever the sample shape, takes place in the presence of PHA depolymerase involving two steps: the first step involves the adsorption of the enzymes on the surface by the binding domain of the enzymes and the second step involves the enzymatic cleavage of polymer chains by the active sites of the enzymes [74].

The slight differences in terms of biodegradation between the 3 PHA studied are more complicated to explain since the biodegradation is a combination of physical, chemical and biological phenomena leading to the material dissolution by enzymatic action of microorganisms. More experiments are needed in order to understand the role of the extrinsic (correlated to the medium) and intrinsic (relative to the polymer) parameters influencing the biodegradation process. It might be relevant to identify and quantify the microorganism population which specifically colonizes the microbeads surface during the test [75]. The diversity of microorganisms associated with these different stages of biodegradation is not yet characterized but this is being further explored in order to better understand the mechanisms. Likewise, the surface morphology of the different PHA has also to be studied in order to correlate the surface properties with the colonization and then the biodegradation. In this study, the PHBHV with 3% in HV is the most biodegradable while being the most crystalline compared to the 2 other PHBHHx. This could a priori constitute a surprising result even if some bibliographic data show that the substrate binding domain of the enzyme is capable to bind to the crystalline PHA material. PHA depolymerase being an

enzyme made up of a catalytic domain and a substrate-binding domain, both these domains are connected by a linker domain. Subsequently, the catalytic domain starts to cleave the single crystals which can be enzymatically hydrolyzed [18]. Other parameters relative to PHA will have to be explored as the hydrophilic/hydrophobic balance of the surface as well as the surface porosity. Understanding the mechanism of PHA degradation and the factors that affect its degradation will help the researcher in designing suitable material for the specific needs.

4. Conclusion

The emulsion-evaporation method allowed the preparation of spherical micrometer PHA beads with tunable materials properties, surface morphologies and related degradation behavior. Using different chemical PHA structures, we showed that the different beads have properties and surface morphologies that are governed by the crystalline organization of the polymer chains within the beads, thus able to provide suitable abrasive and mechanical properties for cosmetics applications. Since pollution of aquatic systems by microplastics should be stopped, the degradation behavior of these PHA microbeads were further tested in marine environment. The degradation experiments reveal that the degradation rate and kinetic were even faster than those of cellulose polymer considered as the most biodegradable polymer materials and also suggest the crucial role of the crystalline content in the degradation process of PHA beads. Very interestingly, these PHA particles are stable in the aqueous media commonly used in cosmetics while being rapidly biodegradable in the marine environment. By combining these two behaviors, they thus offer ideal characteristics for the development of microbeads in cosmetics. In addition, tuning the surface morphologies and biodegradable properties of PHA beads, by using different PHA structures, this provides an effective and promising approach to replace conventional plastic beads from formulation in cosmetic products.

Acknowledgments

The authors would like to thank the Bretagne region for its financial support in this collaborative project called BIOBILLES. The authors are also pleased to express their grateful acknowledgments to Charles-

Henri Morice (Lessonia as industrial partner) and Roland Conanec (Biotech Santé Bretagne as centre for technological innovation) for their contribution to this research program.

References

- [1] N.B. Hartmann, T. Hüffer, R.C. Thompson, M. Hassellöv, A. Verschoor, A.E. Daugaard, S. Rist, T. Karlsson, N. Brennholt, M. Cole, M.P. Herrling, M.C. Hess, N.P. Ivleva, A.L. Lusher, M. Wagner, Are We Speaking the Same Language? Recommendations for a Definition and Categorization Framework for Plastic Debris, *Environmental Science & Technology* 53(3) (2019) 1039-1047.
- [2] Q. Sun, S.-Y. Ren, H.-G. Ni, Incidence of microplastics in personal care products: An appreciable part of plastic pollution, *Science of The Total Environment* 742 (2020) 140218.
- [3] T. Gouin, J. Avalos, I. Brunning, K. Brzuska, J. de Graaf, J. Kaumanns, T. Koning, M. Meyberg, K. Rettinger, H. Schlatter, Use of micro-plastic beads in cosmetic products in Europe and their estimated emissions to the North Sea environment, *SOFW J* 141(4) (2015) 40-46.
- [4] A.S. Tagg, J.A. Ivar do Sul, Is this your glitter? An overlooked but potentially environmentally-valuable microplastic, *Marine Pollution Bulletin* 146 (2019) 50-53.
- [5] S.M. Praveena, S.N.M. Shaifuddin, S. Akizuki, Exploration of microplastics from personal care and cosmetic products and its estimated emissions to marine environment: An evidence from Malaysia, *Marine Pollution Bulletin* 136 (2018) 135-140.
- [6] K. Lei, F. Qiao, Q. Liu, Z. Wei, H. Qi, S. Cui, X. Yue, Y. Deng, L. An, Microplastics releasing from personal care and cosmetic products in China, *Marine Pollution Bulletin* 123(1) (2017) 122-126.
- [7] I.E. Napper, A. Bakir, S.J. Rowland, R.C. Thompson, Characterisation, quantity and sorptive properties of microplastics extracted from cosmetics, *Marine Pollution Bulletin* 99(1) (2015) 178-185.
- [8] V. Godoy, M.A. Martín-Lara, M. Calero, G. Blázquez, Physical-chemical characterization of microplastics present in some exfoliating products from Spain, *Marine Pollution Bulletin* 139 (2019) 91-99.
- [9] A. Piotrowska, O. Czerwińska-Ledwig, M. Serdiuk, K. Serdiuk, W. Pilch, Composition of scrub-type cosmetics from the perspective of product ecology and microplastic content, *Toxicology Environmental Health Sciences* (2020) 1-7.
- [10] E. Kentin, H. Kaarto, An EU ban on microplastics in cosmetic products and the right to regulate, *Review of European, Comparative & International Environmental Law* 27(3) (2018) 254-266.
- [11] L. Anagnosti, A. Varvaresou, P. Pavlou, E. Protopapa, V. Carayanni, Worldwide actions against plastic pollution from microbeads and microplastics in cosmetics focusing on European policies. Has the issue been handled effectively?, *Marine Pollution Bulletin* 162 (2021) 111883.
- [12] C. Guerranti, T. Martellini, G. Perra, C. Scopetani, A. Cincinelli, Microplastics in cosmetics: Environmental issues and needs for global bans, *Environmental Toxicology and Pharmacology* 68 (2019) 75-79.
- [13] R.Z. Habib, M.M. Salim Abdoon, R.M. Al Meqbaali, F. Ghebremedhin, M. Elakashlan, W.F. Kittaneh, N. Cherupurakal, A.-H.I. Mourad, T. Thiemann, R. Al Kindi, Analysis of microbeads in cosmetic products in the United Arab Emirates, *Environmental Pollution* 258 (2020) 113831.
- [14] W. Prus, J. Kozłowska, The influence of new polymeric microbeads in peeling products on skin condition, *Molecular Crystals and Liquid Crystals* 671(1) (2018) 140-147.
- [15] L. da Silva Dutra, T. de Souza Belan Costa, V.T.V. Lobo, T.F. Paiva, M. de Souza Nele, J.C. Pinto, Preparation of Polymer Microparticles Through Non-aqueous Suspension Polycondensations: Part III—Degradation of PBS Microparticles in Different Aqueous Environments, *Journal of Polymers and the Environment* 27(1) (2019) 176-188.
- [16] Y.-K. Hsieh, P.-H. Hung, C.-W. Huang, K.-C. Chuang, J. Wang, Study on the degradation of biodegradable poly (glycerol maleate) (PGM) microbeads, *Polymer Degradation and Stability* 179 (2020) 109223.
- [17] K. Rettinger, B. Huber, Microplastic Particles in Cosmetic Products - Impact on the Environment?, *SOFW J (Proceedings of the 49th Essener Conference)* (2016) 28-32.

469 [18] K. Sudesh, H. Abe, Y. Doi, Synthesis, structure and properties of polyhydroxyalkanoates:
 470 biological polyesters, *Progress in Polymer Science* 25(10) (2000) 1503-1555.

471 [19] Z.A. Raza, S. Abid, I.M. Banat, Polyhydroxyalkanoates: Characteristics, production, recent
 472 developments and applications, *International Biodeterioration & Biodegradation* 126 (2018) 45-56.

473 [20] P. Lemechko, M. Le Fellic, S. Bruzard, Production of poly(3-hydroxybutyrate-co-3-
 474 hydroxyvalerate) using agro-industrial effluents with tunable proportion of 3-hydroxyvalerate monomer
 475 units, *International Journal of Biological Macromolecules* 128 (2019) 429-434.

476 [21] S. Modi, K. Koelling, Y. Vodovotz, Assessment of PHB with varying hydroxyvalerate content for
 477 potential packaging applications, *European Polymer Journal* 47(2) (2011) 179-186.

478 [22] W. Zhao, G.-Q. Chen, Production and characterization of terpolyester poly(3-hydroxybutyrate-co-
 479 3-hydroxyvalerate-co-3-hydroxyhexanoate) by recombinant *Aeromonas hydrophila* 4AK4 harboring
 480 genes *phaAB*, *Process Biochemistry* 42(9) (2007) 1342-1347.

481 [23] G.-Q. Chen, Q. Wu, The application of polyhydroxyalkanoates as tissue engineering materials,
 482 *Biomaterials* 26(33) (2005) 6565-6578.

483 [24] H. Cai, Z. Qiu, Effect of comonomer content on the crystallization kinetics and morphology of
 484 biodegradable poly(3-hydroxybutyrate-co-3-hydroxyhexanoate), *Physical Chemistry Chemical Physics*
 485 11(41) (2009) 9569-9577.

486 [25] Y. Doi, S. Kitamura, H.J.M. Abe, Microbial synthesis and characterization of poly (3-
 487 hydroxybutyrate-co-3-hydroxyhexanoate), 28(14) (1995) 4822-4828.

488 [26] H. Alata, T. Aoyama, Y. Inoue, Effect of Aging on the Mechanical Properties of Poly(3-
 489 hydroxybutyrate-co-3-hydroxyhexanoate), *Macromolecules* 40(13) (2007) 4546-4551.

490 [27] A. Tsui, C.W. Frank, Impact of Processing Temperature and Composition on Foaming of
 491 Biodegradable Poly(hydroxyalkanoate) Blends, *Industrial & Engineering Chemistry Research* 53(41)
 492 (2014) 15896-15908.

493 [28] X.-H. Qu, Q. Wu, J. Liang, B. Zou, G.-Q. Chen, Effect of 3-hydroxyhexanoate content in poly(3-
 494 hydroxybutyrate-co-3-hydroxyhexanoate) on in vitro growth and differentiation of smooth muscle cells,
 495 *Biomaterials* 27(15) (2006) 2944-2950.

496 [29] V.D. Alves, C.A.V. Torres, F. Freitas, Bacterial polymers as materials for the development of
 497 micro/nanoparticles, *International Journal of Polymeric Materials and Polymeric Biomaterials* 65(5)
 498 (2016) 211-224.

499 [30] S.L. Duraikkannu, R. Castro-Muñoz, A. Figoli, A review on phase-inversion technique-based
 500 polymer microsphere fabrication, *Colloid and Interface Science Communications* 40 (2021) 100329.

501 [31] Y. Farrag, W. Ide, B. Montero, M. Rico, S. Rodríguez-Llamazares, L. Barral, R. Bouza, Preparation
 502 of starch nanoparticles loaded with quercetin using nanoprecipitation technique, *International Journal*
 503 *of Biological Macromolecules* 114 (2018) 426-433.

504 [32] A. Rodríguez-Contreras, C. Canal, M. Calafell-Monfort, M.-P. Ginebra, G. Julio-Moran, M.-S.
 505 Marqués-Calvo, Methods for the preparation of doxycycline-loaded phb micro- and nano-spheres,
 506 *European Polymer Journal* 49(11) (2013) 3501-3511.

507 [33] R. Bouza, M. del Mar Castro, S. Dopico-García, M. Victoria González-Rodríguez, L.F. Barral, B.
 508 Bittmann, Polylactic acid and poly(3-hydroxybutyrate-co-3-hydroxyvalerate) nano and microparticles
 509 for packaging bioplastic composites, *Polymer Bulletin* 73(12) (2016) 3485-3502.

510 [34] S. Wohlfart, S. Gelperina, J. Kreuter, Transport of drugs across the blood-brain barrier by
 511 nanoparticles, *Journal of Controlled Release* 161(2) (2012) 264-273.

512 [35] J.L. Maia, M.H.A. Santana, M.I. Ré, The effect of some processing conditions on the characteristics
 513 of biodegradable microspheres obtained by an emulsion solvent evaporation process, *Brazilian Journal*
 514 *of Chemical Engineering* 21 (2004) 01-12.

515 [36] N.L. Zalloum, G. Albino de Souza, T.D. Martins, Single-Emulsion P(HB-HV) Microsphere
 516 Preparation Tuned by Copolymer Molar Mass and Additive Interaction, *ACS Omega* 4(5) (2019) 8122-
 517 8135.

518 [37] V. Deepak, S.b. Ram Kumar Pandian, K. Kalishwaralal, S. Gurunathan, Purification,
 519 immobilization, and characterization of nattokinase on PHB nanoparticles, *Bioresource Technology*
 520 100(24) (2009) 6644-6646.

521 [38] G.A. Senhorini, S.F. Zawadzki, P.V. Farago, S.M.W. Zanin, F.A. Marques, Microparticles of
 522 poly(hydroxybutyrate-co-hydroxyvalerate) loaded with andiroba oil: Preparation and characterization,
 523 *Materials Science and Engineering: C* 32(5) (2012) 1121-1126.

- [39] P.A. Coimbra, H.C.D. Sousa, M.H. Gil, Preparation and characterization of flurbiprofen-loaded poly(3-hydroxybutyrate-co-3-hydroxyvalerate) microspheres, *Journal of Microencapsulation* 25(3) (2008) 170-178.
- [40] Z. Teixeira, N. Durán, S.S. Guterres, Annatto Polymeric Microparticles: Natural Product Encapsulation by the Emulsion–Solvent Evaporation Method, *Journal of Chemical Education* 85(7) (2008) 946.
- [41] W.-C. Hsieh, P.-K. Lin, L.-H. Lin, C.-F. Huang, Flow cytometry analysis using at the poly(3-hydroxybutyrate-co-3-hydroxyvalerate) microspheres for drug delivery system, *Journal of the Taiwan Institute of Chemical Engineers* 44(5) (2013) 829-835.
- [42] J. Chen, S.S. Davis, The release of diazepam from poly(hydroxybutyrate-hydroxyvalerate) microspheres, *Journal of Microencapsulation* 19(2) (2002) 191-201.
- [43] N. Durán, M.A. Alvarenga, E.C. Da Silva, P.S. Melo, P.D. Marcato, Microencapsulation of antibiotic rifampicin in poly(3-hydroxybutyrate-co-3-hydroxyvalerate), *Archives of Pharmacal Research* 31(11) (2008) 1509-1516.
- [44] D. Sendil, I. Gürsel, D. L. Wise, V. Hasırcı, Antibiotic release from biodegradable PHBV microparticles, *Journal of Controlled Release* 59(2) (1999) 207-217.
- [45] J. Hui, X.J. Yu, Y. Zhang, F.Q. Hu, Characterization of anti-cancer drug materials loaded poly (3-hydroxybutyrate-co-3-hydroxyhexanoate) microspheres for drug delivery system in biochemical material system, *Advanced Materials Research, Trans Tech Publ*, 2012, pp. 137-143.
- [46] S. Cheng, Q. Wu, Y. Zhao, B. Zou, G.-Q. Chen, Effect of poly(hydroxybutyrate-co-hydroxyhexanoate) microparticles on growth of murine fibroblast L929 cells, *Polymer Degradation and Stability* 91(12) (2006) 3191-3196.
- [47] A. Chikh, A. Benhamida, M. Kaci, A. Bourmaud, S. Bruzaud, Recyclability assessment of poly(3-hydroxybutyrate-co-3-hydroxyvalerate)/poly(butylene succinate) blends: Combined influence of sepiolite and compatibilizer, *Polymer Degradation and Stability* 142 (2017) 234-243.
- [48] N. Dehouche, C. Idres, M. Kaci, I. Zembouai, S. Bruzaud, Effects of various surface treatments on Aloe Vera fibers used as reinforcement in poly(3-hydroxybutyrate-co-3-hydroxyhexanoate) (PHBHHx) biocomposites, *Polymer Degradation and Stability* 175 (2020) 109131.
- [49] J. Vandewijngaarden, R. Wauters, M. Murariu, P. Dubois, R. Carleer, J. Yperman, J. D'Haen, B. Ruttens, S. Schreurs, N. Lepot, R. Peeters, M. Buntinx, Poly(3-hydroxybutyrate-co-3-hydroxyhexanoate)/Organomodified Montmorillonite Nanocomposites for Potential Food Packaging Applications, *Journal of Polymers and the Environment* 24(2) (2016) 104-118.
- [50] H. Sashiwa, R. Fukuda, T. Okura, S. Sato, A.J.M.d. Nakayama, Microbial degradation behavior in seawater of polyester blends containing poly (3-hydroxybutyrate-co-3-hydroxyhexanoate)(PHBHHx), *Marine drugs* 16(1) (2018) 34.
- [51] I. Zembouai, M. Kaci, L. Zaidi, S. Bruzaud, Combined effects of Sepiolite and Cloisite 30B on morphology and properties of poly(3-hydroxybutyrate-co-3-hydroxyvalerate)/polylactide blends, *Polymer Degradation and Stability* 153 (2018) 47-52.
- [52] T.R. Rigolin, L.C. Costa, T. Venâncio, B. Perlatti, S.H.P. Bettini, The effect of different peroxides on physical and chemical properties of poly(lactic acid) modified with maleic anhydride, *Polymer* 179 (2019) 121669.
- [53] M. Wrona, M.J. Cran, C. Nerín, S.W. Bigger, Development and characterisation of HPMC films containing PLA nanoparticles loaded with green tea extract for food packaging applications, *Carbohydrate Polymers* 156 (2017) 108-117.
- [54] I. Zembouai, M. Kaci, S. Bruzaud, L. Dumazert, A. Bourmaud, M. Mahlous, J.M. Lopez-Cuesta, Y. Grohens, Gamma irradiation effects on morphology and properties of PHBV/PLA blends in presence of compatibilizer and Cloisite 30B, *Polymer Testing* 49 (2016) 29-37.
- [55] S. Bruzaud, A. Bourmaud, Thermal degradation and (nano)mechanical behavior of layered silicate reinforced poly(3-hydroxybutyrate-co-3-hydroxyvalerate) nanocomposites, *Polymer Testing* 26(5) (2007) 652-659.
- [56] W.C. Oliver, G.M. Pharr, An improved technique for determining hardness and elastic modulus using load and displacement sensing indentation experiments, *Journal of Materials Research* 7(6) (1992) 1564-1583.

- [57] M. Deroiné, G. César, A. Le Duigou, P. Davies, S. Bruzard, Natural Degradation and Biodegradation of Poly(3-Hydroxybutyrate-co-3-Hydroxyvalerate) in Liquid and Solid Marine Environments, *Journal of Polymers and the Environment* 23(4) (2015) 493-505.
- [58] D.P. Pacheco, M.H. Amaral, R.L. Reis, A.P. Marques, V.M. Correló, Development of an injectable PHBV microparticles-GG hydrogel hybrid system for regenerative medicine, *International Journal of Pharmaceutics* 478(1) (2015) 398-408.
- [59] J. Bidone, A.P.P. Melo, G.C. Bazzo, F. Carmignan, M.S. Soldi, A.T.N. Pires, E. Lemos-Senna, Preparation and characterization of ibuprofen-loaded microspheres consisting of poly(3-hydroxybutyrate) and methoxy poly (ethylene glycol)-b-poly (D,L-lactide) blends or poly(3-hydroxybutyrate) and gelatin composites for controlled drug release, *Materials Science and Engineering: C* 29(2) (2009) 588-593.
- [60] J.-W. You, H.-J. Chiu, W.-J. Shu, T.-M. Don, Influence of Hydroxyvalerate Content on the Crystallization Kinetics of Poly(hydroxybutyrate-co-hydroxyvalerate), *Journal of Polymer Research* 10(1) (2003) 47-54.
- [61] Y. Kann, M. Shurgalin, R.K. Krishnaswamy, FTIR spectroscopy for analysis of crystallinity of poly(3-hydroxybutyrate-co-4-hydroxybutyrate) polymers and its utilization in evaluation of aging, orientation and composition, *Polymer Testing* 40 (2014) 218-224.
- [62] J. Xu, B.-H. Guo, R. Yang, Q. Wu, G.-Q. Chen, Z.-M. Zhang, In situ FTIR study on melting and crystallization of polyhydroxyalkanoates, *Polymer* 43(25) (2002) 6893-6899.
- [63] S.-G. Hong, W.-M. Chen, The Attenuated Total Reflection Infrared Analysis of Surface Crystallinity of Polyhydroxyalkanoates e-Polymers 6(1) (2006).
- [64] N. Vasanthan, D.R. Salem, FTIR spectroscopic characterization of structural changes in polyamide-6 fibers during annealing and drawing, *Journal of Polymer Science Part B: Polymer Physics* 39(5) (2001) 536-547.
- [65] M. Kansiz, A. Domínguez-Vidal, D. McNaughton, B. Lendl, Fourier-transform infrared (FTIR) spectroscopy for monitoring and determining the degree of crystallisation of polyhydroxyalkanoates (PHAs), *Analytical and Bioanalytical Chemistry* 388(5) (2007) 1207-1213.
- [66] A. Padermshoke, H. Sato, Y. Katsumoto, S. Ekgasit, I. Noda, Y. Ozaki, Thermally induced phase transition of poly(3-hydroxybutyrate-co-3-hydroxyhexanoate) investigated by two-dimensional infrared correlation spectroscopy, *Vibrational Spectroscopy* 36(2) (2004) 241-249.
- [67] J.S. Lim, K.-i. Park, G.S. Chung, J.H. Kim, Effect of composition ratio on the thermal and physical properties of semicrystalline PLA/PHB-HHx composites, *Materials Science and Engineering: C* 33(4) (2013) 2131-2137.
- [68] D.D. Wright-Charlesworth, D.M. Miller, I. Miskioglu, J.A. King, Nanoindentation of injection molded PLA and self-reinforced composite PLA after in vitro conditioning for three months, *74A(3)* (2005) 388-396.
- [69] G.Z. Voyiadjis, A. Samadi-Dooki, L. Malekmoie, Nanoindentation of high performance semicrystalline polymers: A case study on PEEK, *Polymer Testing* 61 (2017) 57-64.
- [70] I. Ovchinnikov, A. Vishnevskiy, D. Seregin, A. Rezvanov, D. Schneider, A. Sigov, K.A. Vorotilov, M. Baklanov, Evaluation of mechanical properties of porous OSG films by PFQNM AFM and benchmarking with traditional instrumentation, *Langmuir* 36(32) (2020) 9377-9387.
- [71] A. Flores, F. Ania, F. Baltá-Calleja, From the glassy state to ordered polymer structures: A microhardness study, *Polymer* 50(3) (2009) 729-746.
- [72] M. Deroiné, A. Le Duigou, Y.-M. Corre, P.-Y. Le Gac, P. Davies, G. César, S. Bruzard, Accelerated ageing of polylactide in aqueous environments: Comparative study between distilled water and seawater, *Polymer Degradation and Stability* 108 (2014) 319-329.
- [73] D. Jendrossek, O. Selchow, M. Hoppert, Poly(3-Hydroxybutyrate) Granules at the Early Stages of Formation Are Localized Close to the Cytoplasmic Membrane in *Caryophanon latum*, *Applied and Environmental Microbiology* 73(2) (2007) 586.
- [74] K. Numata, H. Abe, Y. Doi, Enzymatic processes for biodegradation of poly(hydroxyalkanoate)s crystals, *Canadian Journal of Chemistry* 86(6) (2008) 471-483.
- [75] C. Dussud, C. Hudec, M. George, P. Fabre, P. Higgs, S. Bruzard, A.-M. Delort, B. Eyheraguibel, A.-L. Meistertzheim, J. Jacquin, J. Cheng, N. Callac, C. Odobel, S. Rabouille, J.-F. Ghiglione, Colonization of Non-biodegradable and Biodegradable Plastics by Marine Microorganisms, *Frontiers in microbiology* 9(1571) (2018).

Figures

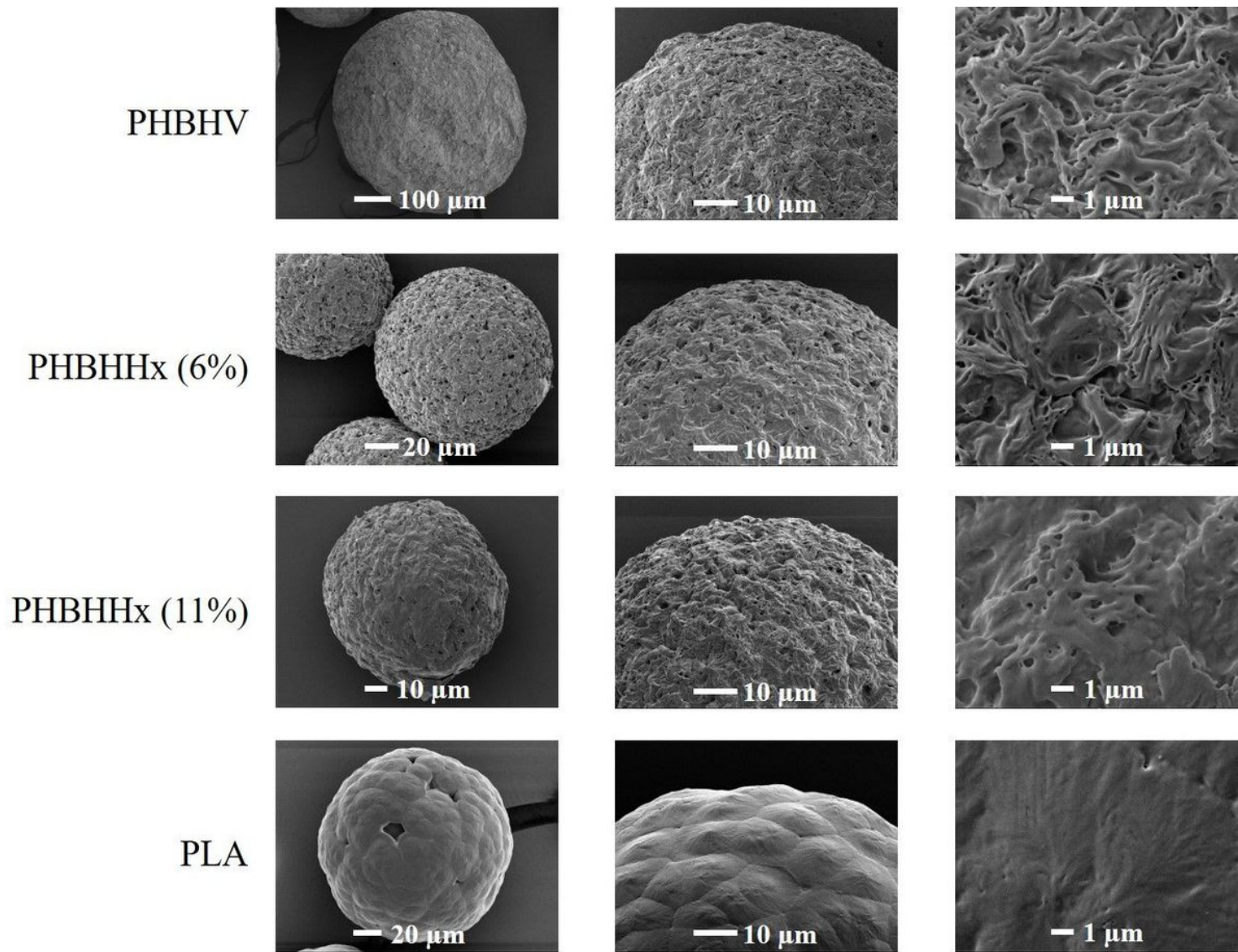


Figure 1

SEM images of the different microbeads are presented in Figure 1.

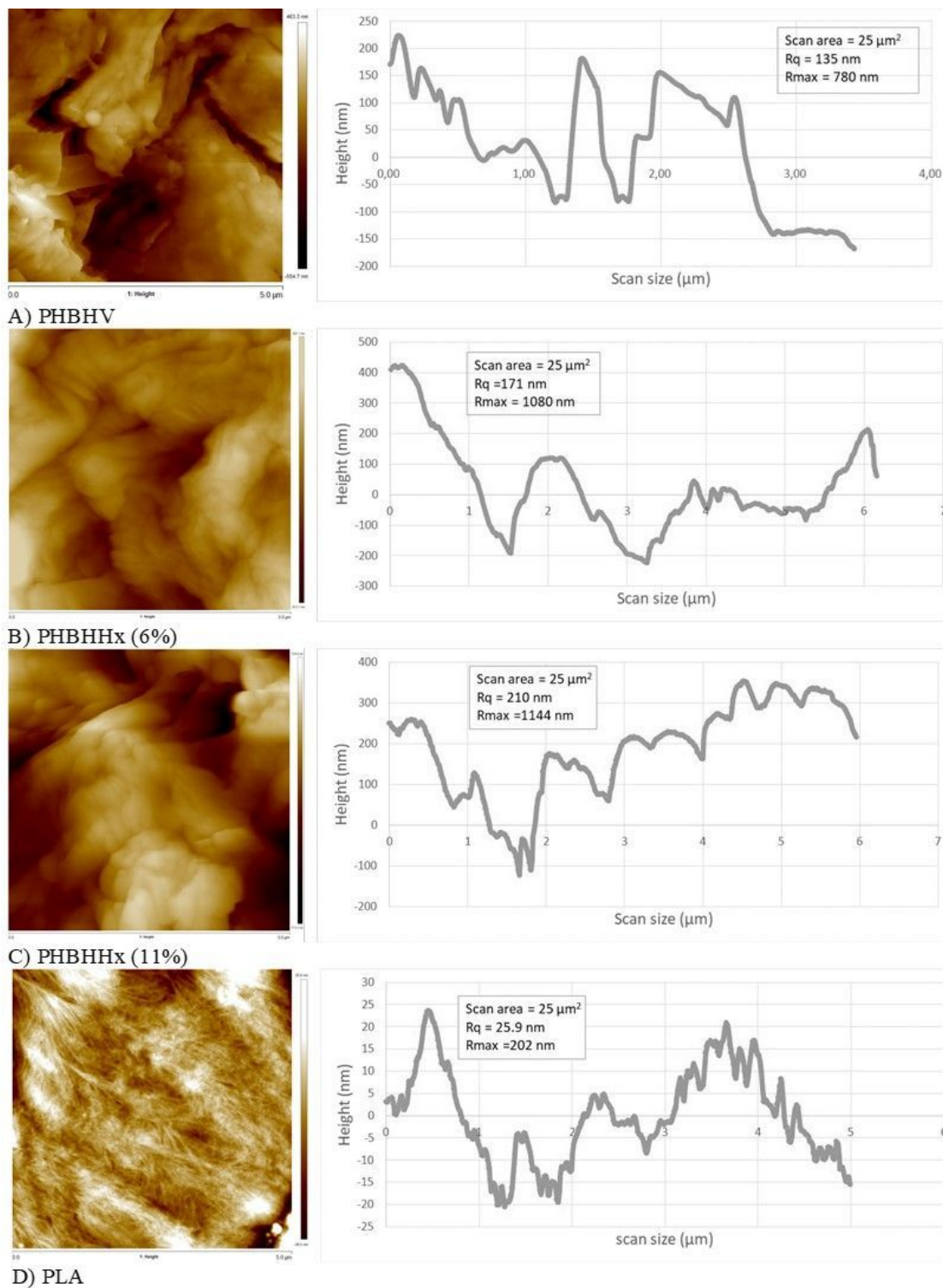
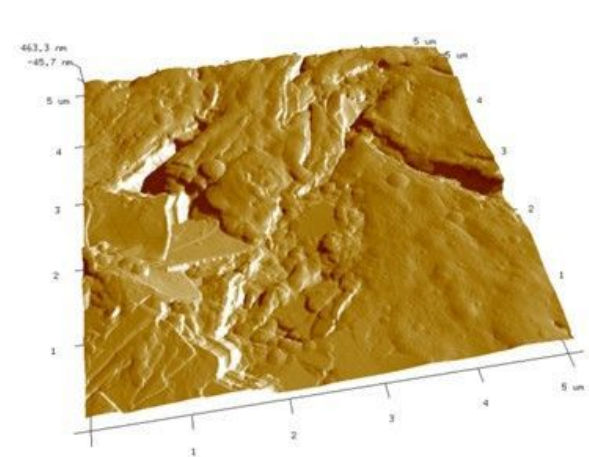
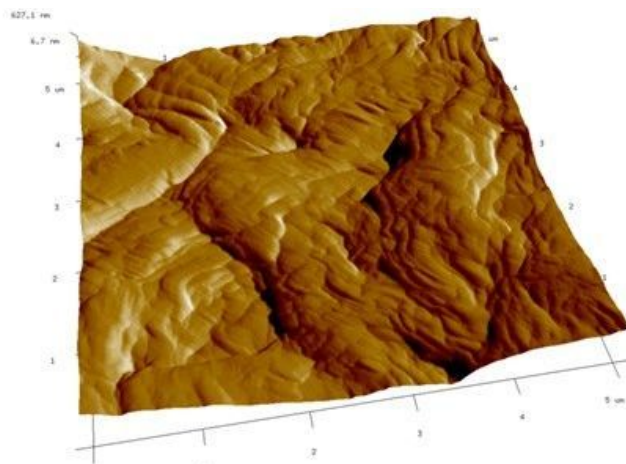


Figure 2

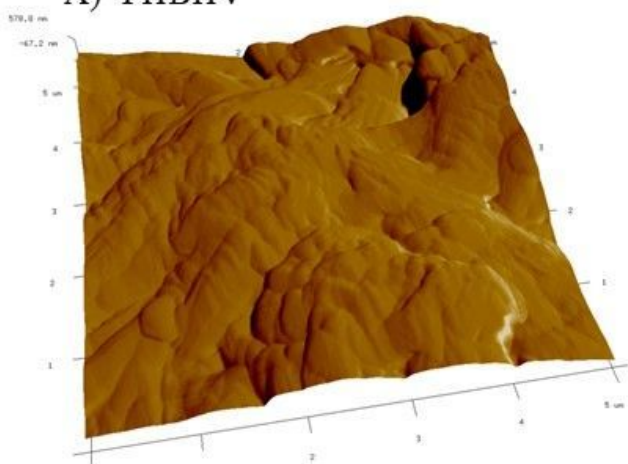
Figure 2 presents AFM images obtained of the top of the different beads and their corresponding surface analysis, confirming the smooth topography of the PLA beads and the important roughness of the PHA beads.



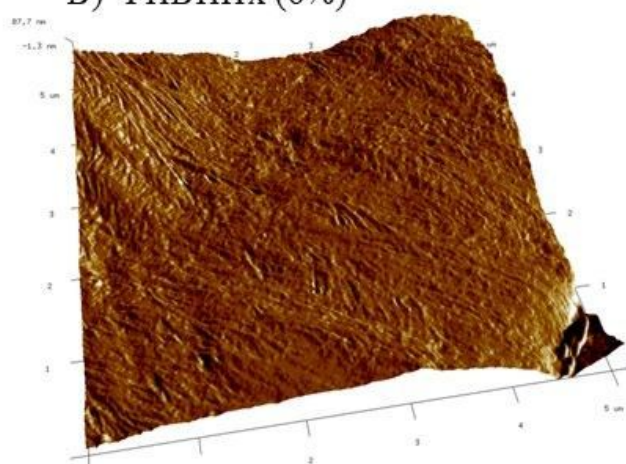
A) PHBHV



B) PHBHHx (6%)



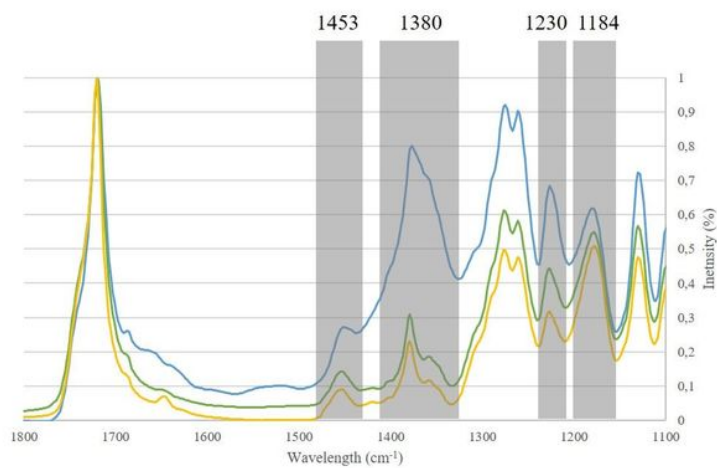
C) PHBHHx (11%)



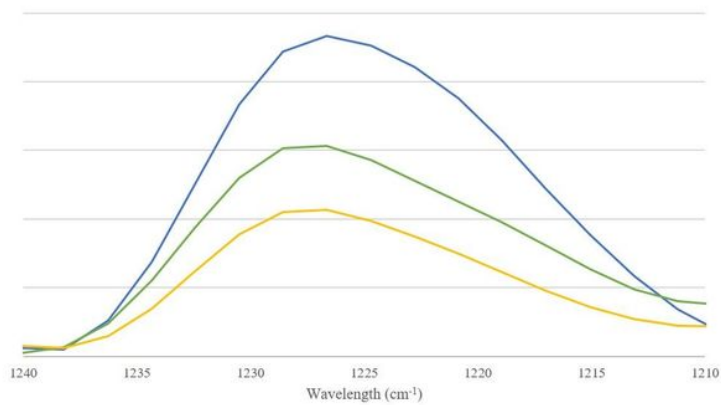
D) PLA

Figure 3

Microparticles of PHBHV, PHBHHx (6% and 11%) and PLA were elaborated by emulsification process. PHBHV was dissolved at 50 g L⁻¹ in chloroform under reflux conditions (50 °C), PHBHHx and PLA were dissolved at the same concentration but in dichloromethane under reflux conditions (40 °C) during 24 hours.



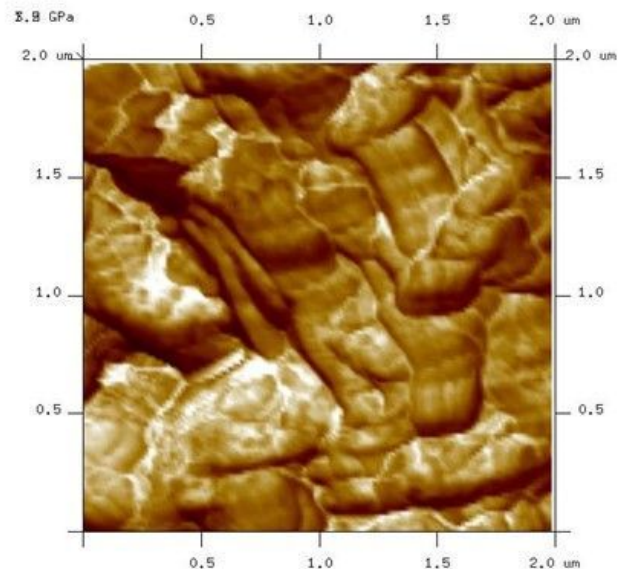
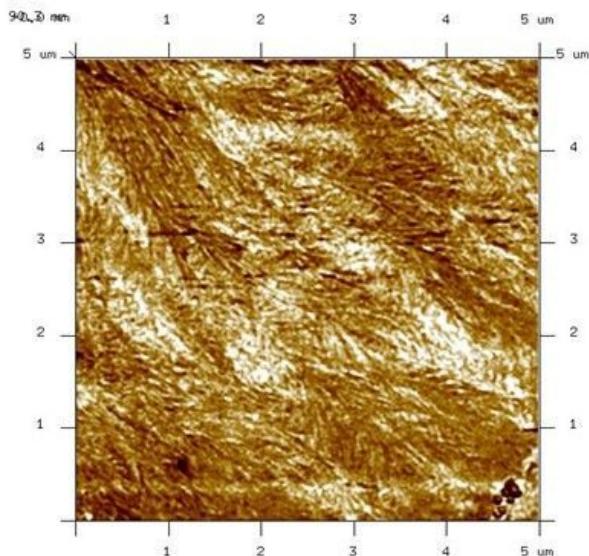
A



B

Figure 4

Figure 4 represents an IR spectrum of the PHA microbeads and reveals the different bands of interest for this polymer.



PLA, Indentation Modulus = 6.05 ± 0.51 GPa

PHBV, Indentation Modulus = 7.02 ± 2.64 GPa

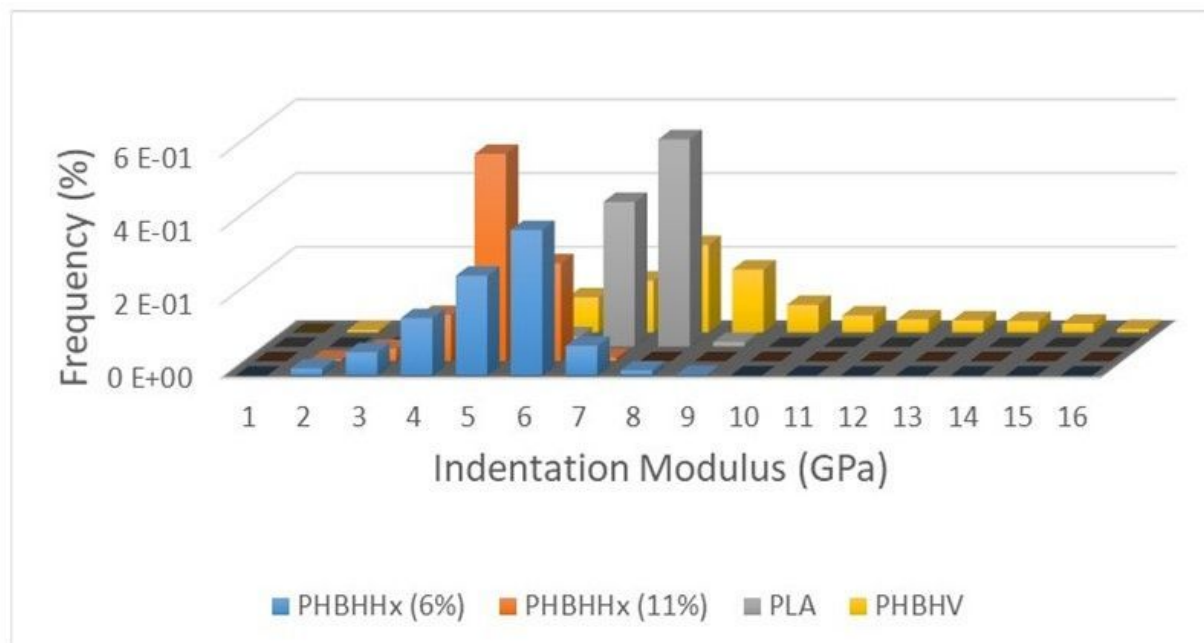


Figure 5

Figure 5 represents the distribution in the indentation modulus for the different beads as measured by PFQNM. Results obtained are consistent with the moduli obtained by nanoindentation.

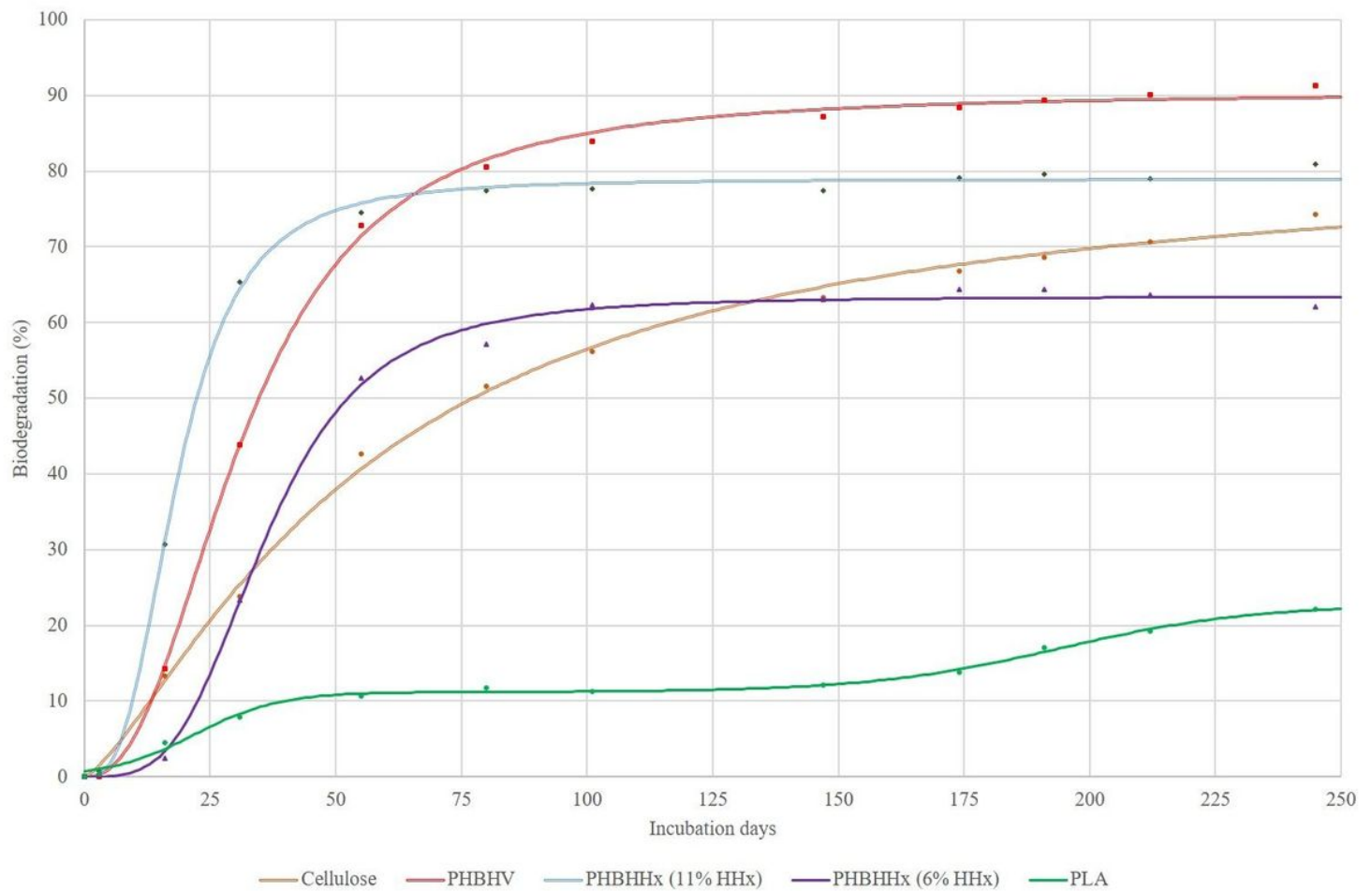


Figure 6

The Figure 6 shows the biodegradability of the different microbeads in seawater. The biodegradation has been performed on marine environment (seawater + sediments) at 25 °C, according to the NF EN ISO 19679 standard.